Hindawi
Adsorption Science & Technology
Volume 2023, Article ID 7228408, 9 pages
https://doi.org/10.1155/2023/7228408

Research Article

Optimization of Activated Carbon Fiber Preparation from Hemp Fiber through Dipotassium Hydrogen Phosphate for Application of Thermal Storage System

L. Natrayan,[1] **S. Kaliappan**,[2] **S. Chinnasamy Subramanian**,[3] **Pravin P. Patil**,[4] **S. D. Sekar**,[5] **Y. Sesha Rao**,[6] **and Melkamu Beyene Bayu**[7]

[1]*Department of Mechanical Engineering, Saveetha School of Engineering, SIMATS, 602 105, Chennai, Tamil Nadu, India*
[2]*Department of Mechanical Engineering, Velammal Institute of Technology, Chennai, 601204 Tamil Nadu, India*
[3]*Department of Mechanical Engineering, Velammal Engineering College, Chennai, 66 Tamil Nadu, India*
[4]*Department of Mechanical Engineering, Graphic Era Deemed to be University, Bell Road, Clement Town, 248002 Dehradun, Uttarakhand, India*
[5]*R. M. K. Engineering College, R. S. M. Nagar, Kavaraipettai 601206, Gummidipoondi Taluk, Thiruvallur District, Tamil Nadu, India*
[6]*Department of Mechanical Engineering, QIS College of Engineering and Technology, Ongole, Andhra Pradesh, India*
[7]*Department of Mechanical Engineering, Ambo Institute of Technology-19, Ambo University, Ethiopia*

Correspondence should be addressed to Melkamu Beyene Bayu; melkamu.beyene@ambou.edu.et

Received 13 October 2022; Revised 22 March 2023; Accepted 4 April 2023; Published 21 April 2023

Academic Editor: Debabrata Barik

With significant benefits over many other commercialised thermal storage methods, activated carbon fiber (ACF) is believed to be among the finest biosorbents for adsorbent purposes. If correctly made, it is an outstanding mesoporous lightweight material with micropores and, in most cases, no micropores. ACF's higher bulk densities and great dynamic capacity demonstrate its value and are used in adsorbent technologies. The present study's primary goal is to create active carbon fiber from organic hemp fiber. The following parameters were selected: (i) activating temperatures, (ii) activating timing, (iii) carbonization temperature, (iv) activating ingredient %ages, and (v) speed of activation temperature, all with four levels to achieve the goal. Taguchi optimization techniques were used to optimize the adsorbent characteristics. The current study used an L16 orthogonal array to accomplish that improvement. According to the previous Taguchi, the optimal conditions were 300°C combustions, insemination with 22.5% *w*/*v* K_2HPO_4 solution, and activating at 800°C for 3 hours at 20°C/min. The greatest contribution is 54.75%, followed by the rate of temperature activation at 23.35%, carbonated temperature at 10.14%, duration of stimulation at 8.82%, and H_3PO_4 concentrations at 2.94%. The results show that the activation temperature and rate of the temperature of activations are the essential elements in the current study's accomplishment of the best adsorption capacities.

1. Introduction

Environmental contamination is a severe adverse effect of the modern country's fast economic expansion. Industrial effluent, in particular, poses significant problems, if not a catastrophe, due to its massive flow, increased nutrient concentration, intense hue, and complex breakdown [1, 2]. As a result, eliminating dye effluent is a critical challenge for industrialization. Membrane filtration, electrodynamics, and photocatalyst innovation have all been shown to be effective for sophisticated wastewater purification. Furthermore, the above procedures have certain limitations, including complexity, high price, and limited purifying effectiveness [3, 4]. Apart from the strategies mentioned previously, the physiological adsorption process has received increasing attention in the use of dyeing for sewage decontamination due to its high sorption performance and low technological hurdles. Because of their rich porous structure, high surface area, and diversity of established groups, active carbon fibers (ACFs) are regarded as effective adsorbents [5].

As a result, various ACFs were documented to be used in the filtration of printed and dyed effluent. In earlier studies, synthetic fibers such as PAN (polyacrylonitrile) and cellulosic were used as precursor materials to produce active carbon fibers with outstanding adsorption efficiency for metal ions and specific molecular pigments. Furthermore, undesired deterioration has hampered the progress of such chemically bonded ACFs [6, 7].

Biocomposite substances have lately gained popularity as a response to the disposal site crisis, the depletion of oil supplies and worries about emissions produced by their use. These comprise sustainable agricultural production fuel sources such as timber, agricultural residues, and plant-origin fibers [8, 9]. Hence, the need to create activated carbon adsorbent materials with low-cost, high-efficiency alternative antecedents. As a result of their minimal price, recyclability, and willingness to contract, natural fabrics are among the different scenarios [10]. Activated carbons were prepared using natural materials like hemp fiber, oil palm fiber, linen, and kenaf. Natural materials are divided into three groups based on their source within the tree: the thickest, leaves, and germ fibers. Bast fibers include cotton, jute, wheat, and flax. Bast fibers are widely used in the production of cables and monumental manufacturing textiles [11, 12]. Hemp fiber is commonly used for membranifaciens, specialised textile materials like mainsail and napkins, and specialised printing like tea paper and Starbucks filtration. Leaf fibers include jute, bananas, coconut, and pineapple [13, 14].

Due to its cost-effectiveness, limited technological obstacles, and long-term benefits, considerable effort has been made to manufacture active carbon fibers from biomasses, particularly biological residuals like lemon peel, stems, and disposal residuals from extraction minerals [15, 16]. Furthermore, active carbon fibers from renewable sources opened up a new avenue for the elevated exploitation of biowaste. Moreover, the adsorption rate of activated charcoal fiber biorenewable resources varies greatly, with consternation carbon fiber exhibiting the highest adsorption capability (165210 mg/g for methylene blue), implying that the microhardness of organic matter fiber has a significant effect on carbon fiber achievement [17, 18]. Moreover, the reaction mechanism in the production of carbon fiber is an essential factor that affects carbon composite sorption capacity; additionally, comprehensive activation, supplementary initiation, and surface coating consolidated reaction mechanisms are all helpful for increasing carbon fiber adsorption efficiency [19].

Adsorbents utilising heterogeneous catalysts are a simple and effective strategy to remove a wide range of natural and artificial contaminants from sewage. There are three techniques for producing activated charcoal. The catalytic cracking of a precursor in an innocuous flow at temperatures up from 500 to 1000 degrees Celsius results in char creation [20, 21]. The charcoal is then ignited in an oxidising gas like carbon dioxide and vapour at temperatures ranging from 700 to 1300 degrees Celsius. Enzymatic hydrolysis entails impregnating a prelude with oxidising reagents like K_2CO_3, $ZnCl_2$, H_3PO_4, $AlCl_3$, and Na_2HPO4 and burning them in a neutral gas like nitrogen or argon gas [22, 23]. The biophysical activating approach combines physiochemical activating methods. The Taguchi optimization approach could be used to optimize active carbon generation. Taguchi, a simple and effective statistical and analytical strategy, conducts continuous testing to identify near-optimal choices for compensation and efficiency. A high number of parameters may be explored with a minimal number of experimental runs in this manner [3, 4].

The synthesis of active carbon fiber utilising natural hemp materials employing a chemical activation technique was studied in this work. It determined the optimal quantity of every variable in manufacturing activated carbon fiber. The Taguchi design analysis was used to measure the impact of process variables like carbonization temperature, dipotassium hydrogen phosphate composition in the authentication solvent, activation temperature, and activation process on the adsorption capacities of rehearsed adsorbent fiber. The properties and adsorption capabilities of activated carbon fiber produced under optimal circumstances were also studied.

2. Experimental Works

2.1. Materials. Rithu Natural Fiber Industry in Vellore, Tamil Nadu, India, supplied the hemp fiber. Naga Chemical Industry in Chennai, Tamil Nadu, India, supplied the dipotassium hydrogen phosphate. Other compounds have been of analytical quality. All needed formulations were prepared using double-filtered water.

2.2. Activated Carbon Preparations. The primary material for producing active carbon fibers is hemp fiber-based fabric. Cannabis was cleaned with double purified water to eliminate dirt before drying. Dried cannabis specimens weighing 5 g were put in a steel longitudinal tubular furnace. A neutral nitrogen flow was forced through the combustion chamber at a fluid velocity of 75 cm^3/min for 30 min. The oven temperature was increased at an average rate of 20°C/min throughout the combustion process to obtain the different carbonization temperatures indicated by a Taguchi technique [24]. Hemp specimens were maintained at these temperatures for 1 hour. In an N_2 atmosphere, carbonized cannabis samples were washed to ambient temperature. In addition, many hemp specimens were tested without activated carbon. Activated carbon hemp was immersed in a 50 mL K_2HPO_4 solution and left overnight to attain maximal immersion during the chemical transformation [25]. The Taguchi technique suggested the examined %ages of K_2HPO_4 mixtures with different proportions. The soaking carbonized hemp was then dried in a hot air oven at 110°C before being inserted in furnaces. It held for 30 min at room temperature below a nitrogen environment with a fluid velocity of 75 cm^3/min. Following that, the burner was warmed with varying rates of temperature increase and maintained at this level for different periods. The Taguchi approach suggested the activating temperatures, activation process, and probability of obtaining the activating temp. Subsequently, the activated carbon was chilled in an anaerobic environment before being rinsed using solvent and

Table 1: Parameters and their levels.

Sl. No	Parameters	Symbols	Levels			
			L1	L2	L3	L4
1	Temperature of activation (°C)	A	600	700	800	900
2	Rate of temperature activation (°C/min)	B	40	30	20	10
3	H_3PO_4 concentration (w/v)	C	7.5	15	22.5	30
4	Carbonization temperature (°C)	D	Without	200	300	400
5	Time of activation (hrs)	E	1	2	3	4

Table 2: Iodine values of different process parameters on the adsorption.

Sl. No	A	B	C	D	E	Iodine values			S/N values
						X_1	X_2	Mean values	
1	600	40	7.5	Without	1	42.05	51.59	46.82	33.41
2	600	30	15	200	2	134.68	144.22	139.45	42.89
3	600	20	22.5	300	3	193.91	203.45	198.68	45.96
4	600	10	30	400	4	141.86	151.4	146.63	43.32
5	700	40	15	300	4	133.67	143.27	138.47	42.83
6	700	30	7.5	400	3	101.76	111.3	106.53	40.55
7	700	20	30	Without	2	240.6	238.96	239.78	47.60
8	700	10	22.5	200	1	214.95	225.68	220.315	46.86
9	800	40	22.5	400	2	253.1	262.64	257.87	48.23
10	800	30	30	300	1	260.19	259.14	259.665	48.29
11	800	20	7.5	200	4	294.72	304.26	299.49	49.53
12	800	10	15	Without	3	234.47	244.01	239.24	47.58
13	900	40	30	200	3	229.11	238.65	233.88	47.38
14	900	30	22.5	Without	4	181.19	186.54	183.865	45.29
15	900	20	15	400	1	242.34	245.89	244.115	47.75
16	900	10	7.5	300	2	335.59	331.57	333.58	50.46

Table 3: S/N values of adsorption for storage system.

Levels	A	B	C	D	E
1	41.40	47.06	43.49	43.47	44.08
2	44.46	47.71	45.26	46.66	47.29
3	48.41	44.25	46.59	46.89	45.37
4	47.72	42.96	46.65	44.96	45.24
Delta	7.01	4.72	3.16	3.42	3.22
Rank	1	2	5	3	4

afterwards twice filtered water till the pH of a cleaning discharge was achieved.

2.3. Optimization of ACF Preparation Conditions. The Taguchi design approach was utilised to optimize the ACF processibility. An L16 factorial design containing five process variables in four stages was employed to determine the best frequencies. The four stages of every studied operation variable would be as follows: Table 1 displays the different parameters and respective ranges.

Table 1 shows the preparation of 16 distinct ACF specimens using the Taguchi array design concept. The iodine value of every produced ACF specimen was evaluated in double in specified tests as a criterion of the material's adsorption ability. The optimisation criteria were the iodine value of the specimens. To study the effect of operating settings on the adsorption capacities of the produced ACF, the signal-to-noise ratios (S/N ratios) of recorded iodine concentrations were studied using the variance test (ANOVA) approach. Because the improved circumstances correspond to the adsorbent's higher adsorption capabilities, the

Table 4: ANOVA analysis of adsorptions of iodine in phenolic acid.

Source	DF	SOS	Contribution (%)	Adj SS	Adj MS
A	3	45743	54.75	45743	15247.7
B	3	19514	23.35	19514	6504.7
C	3	2453	2.94	2453	817.7
D	3	8472	10.14	8472	2824.1
E	3	7372	8.82	7372	2457.5
Error	0	0	0	0	0
Total	15	83555	100	—	—

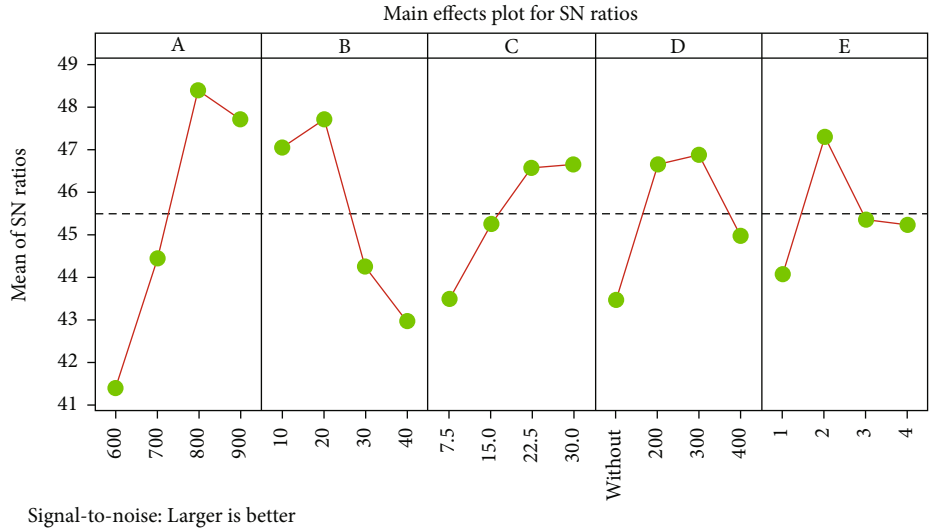

Figure 1: The iodine values of adsorptions based on various input factors.

"bigger-is-better" approach for calculating the S/N ratios was used [3, 8]. The S/N ratio is determined as follows:

$$\text{S/Nratio} = -10 \log_{10} \frac{1}{e} \sum_{a=i}^{e} \frac{1}{X_i}, \quad (1)$$

where e represents the size of replicas and x_i is the iodine value of created ACF specimen in every replicate. Due to the obvious "larger is good" approach, raising the S/N ratio corresponds to raising the adsorption properties of the ACF samples produced. ASTM D4607-94 was used to estimate the iodine value of ACF specimens.

3. Result and Discussion

3.1. Regression-Based Analysis. Based on the different combinations, 16 distinct ACF specimens were generated using the Taguchi technique's L16 array, and the iodine value of every specimen was calculated. Table 2 displays the iodine values and their accompanying S/N combinations. Table 3 shows the delta rank and its accompanying values. Table 4 displays the results of the F-test for S/N proportions. Improving the S/N proportion corresponds to enhancing the adsorption capability of ACF samples generated. Figure 1 shows the iodine values of adsorptions based on various input factors.

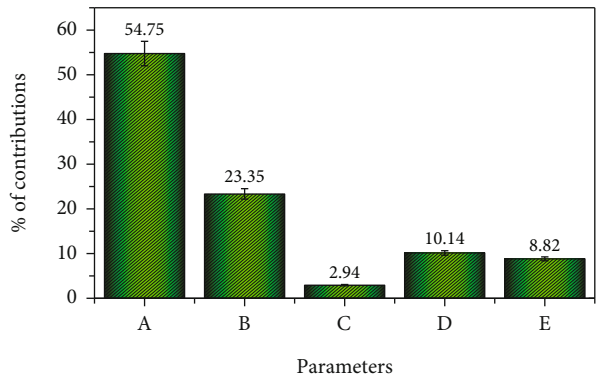

Figure 2: Error plots of percent contributions of various influencing parameters of iodine adsorptions.

3.2. Analysis of Variance. An ANOVA was used to determine the significance of interrupted processing elements. Table 4 provides the %age of contribution for each processing parameter. The process parameter known as the F-test is hypothesised to affect adsorption characteristics. Figure 2

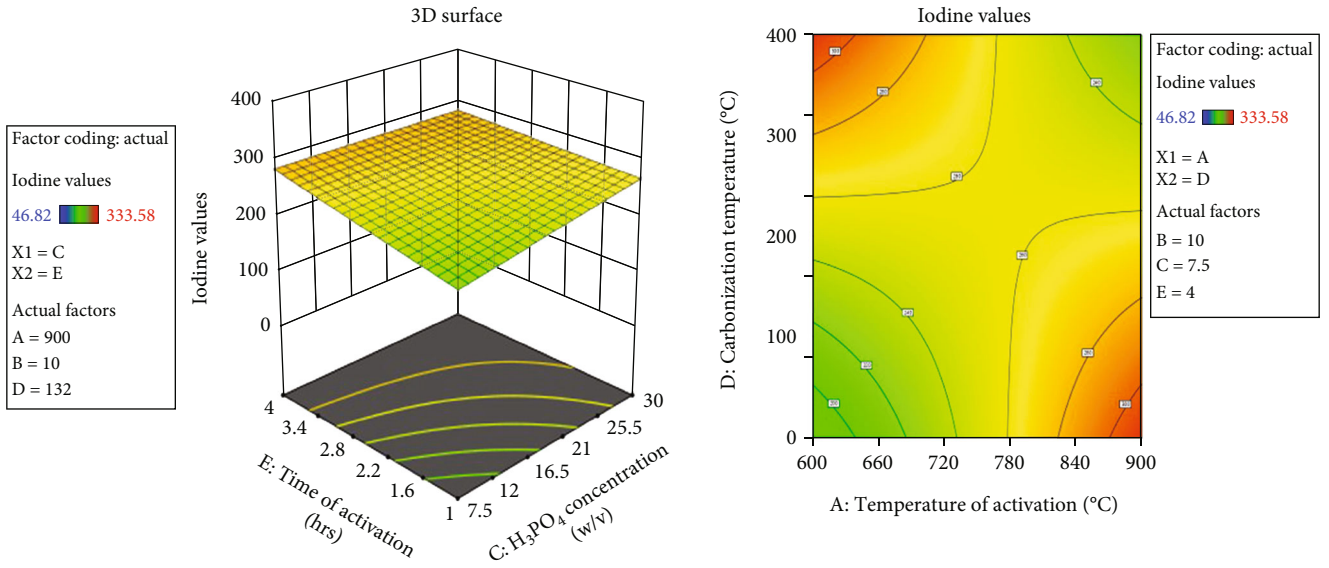

Figure 3: Surface and contour plots of activation temperature based on input parameters.

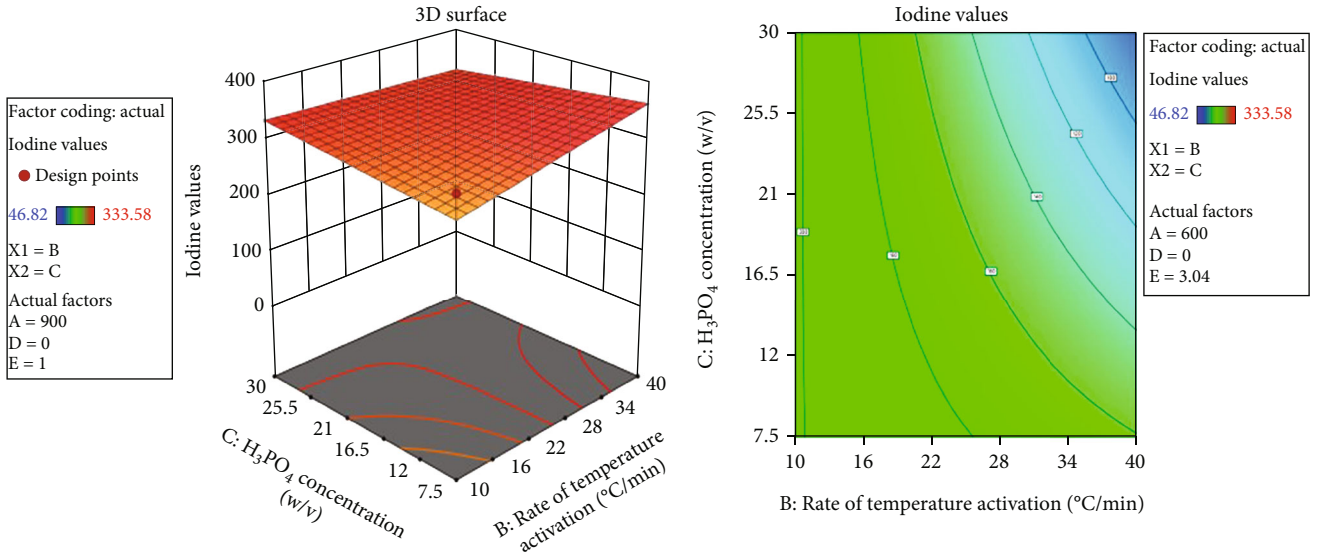

Figure 4: Surface and contour plots of rate of activation temperature based on input parameters.

depicts the %age contribution of each ingredient. The contributory %age is the fraction of the sentencing hearing total variance that considers each meaningful impact [4]. The regressions of current adsorption characteristics are expressed by equation (2).

$$\begin{aligned}\text{Iodine values} = {} & 205.5 - 72.63A1 - 29.25A2 + 58.54A3 \\ & + 43.34A4 + 29.42B1 + 39.99B2 \\ & - 33.15B3 - 36.26B4 - 8.919C1 \\ & - 15.21C2 + 9.659C3 + 14.47C4 \\ & - 28.10D1 + 17.76D2 + 27.07\,D3 \\ & - 16.74D4 - 12.80E1 + 37.15E2 \\ & - 10.94E3 - 1.41E4.\end{aligned} \tag{2}$$

Figure 2 depicts the contribution of processing parameters to adsorption characteristics. Table 4's percent contribution is a controlling factor to attain the highest iodine. The P value specifies the probability of recurrent factors. The most significant contribution is 54.75%, followed by the rate of temperature activation at 23.35%, carbonated temperature at 10.14%, duration of stimulation at 8.82%, and H_3PO_4 concentrations at 2.94%. The results show that the activation temperature and rate of the temperature of activations are the essential elements in the current study's accomplishment of the best adsorption capacities.

4. Impact of Processing Parameters

4.1. Result of Activation Temperature. Raising the activating temperatures to 800°C improves the S/N ratio, implying that

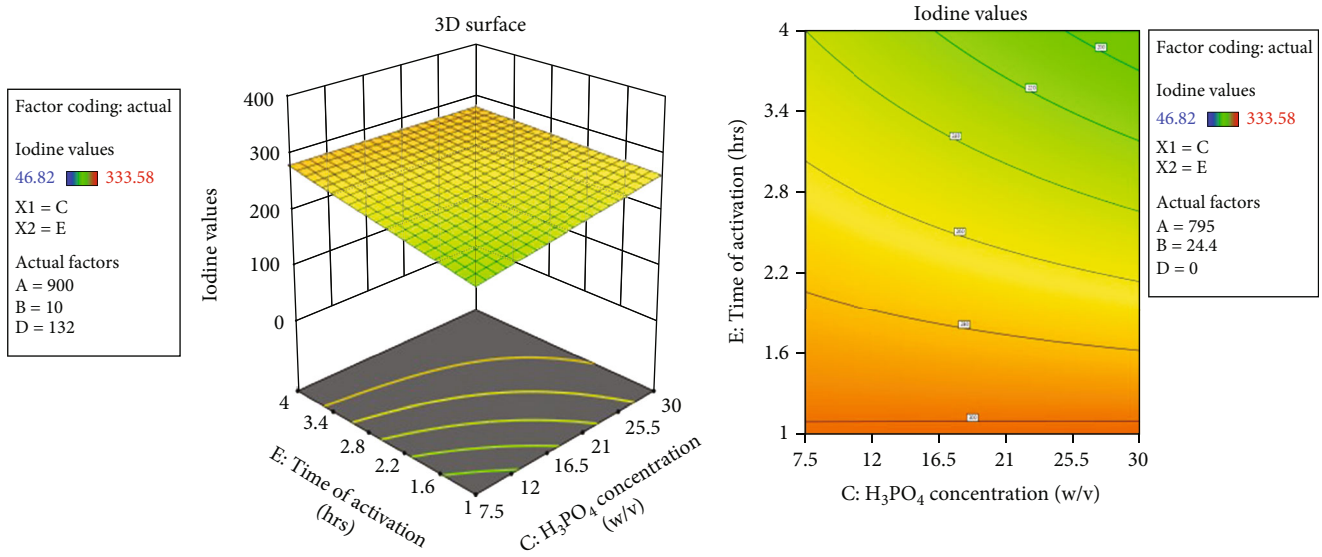

Figure 5: Surface and contour plots of effect of K_2HPO_4 concentration based on input parameters.

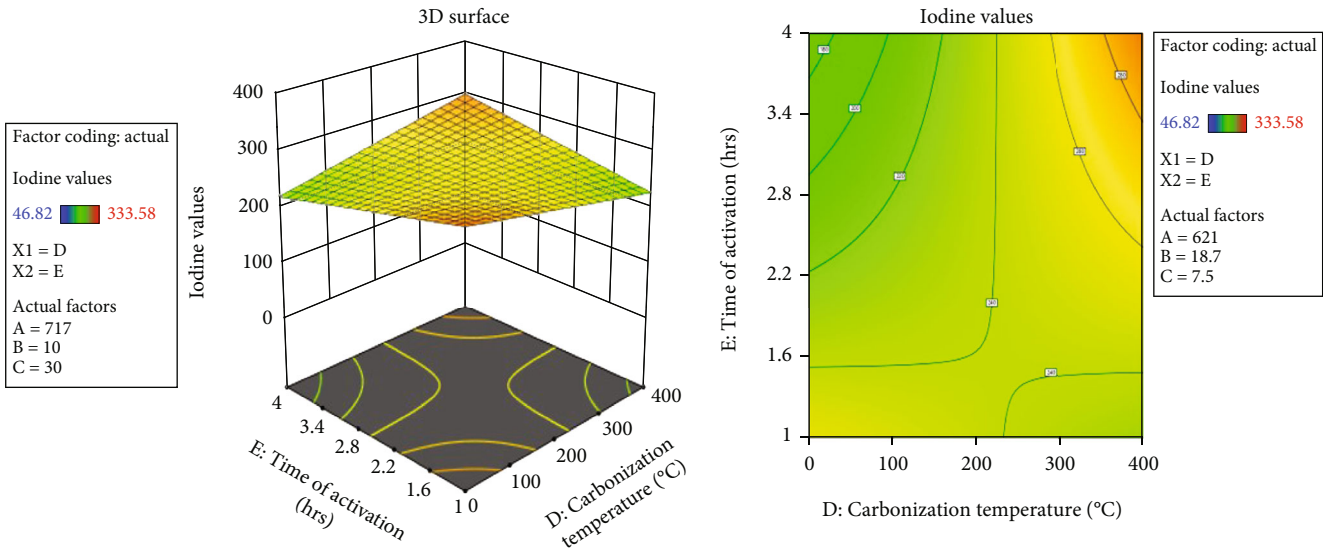

Figure 6: Surface and contour plots of the effect of carbonation temperature based on input parameters.

the adsorption efficiency of ACF specimens improves as the activating temperature increases. This might be attributed to increased activation and small pore creation throughout the processed ACF. Several studies have found similar findings. An elevation in reaction temperature up to 900°C reduces the ACF's adsorption capability. This is most likely due to the loss of the porous structure and the formation of bigger pores that limit the adsorption capability [24, 26]. Figure 3 demonstrates the above findings.

4.2. Consequence of the Level of Attaining the Activation Temperature. Figure 4 indicates that increasing the activating temperature level between 10 and 20°C/min improves the S/N ratio of the generated ACF specimens. This leads to a rise in ACF adsorption, which may be due to decreased degradation of ACF molecules. The ACF structure is most likely destroyed and transformed at excessive temperature increase levels to charcoal [27, 28].

4.3. Effect of K_2HPO_4 Concentration. As shown in Figure 5, increasing the phosphorus potassium dihydrogen level from 7.5 to 22.5% *w/v* increases the S/N ratio of the iodine values in the activated carbon fiber specimens produced. This might be attributed to a rise in the creation of small pores, as in ACF, that are more efficient in the adsorption mechanism and boost absorbent adsorption properties. Surpassing

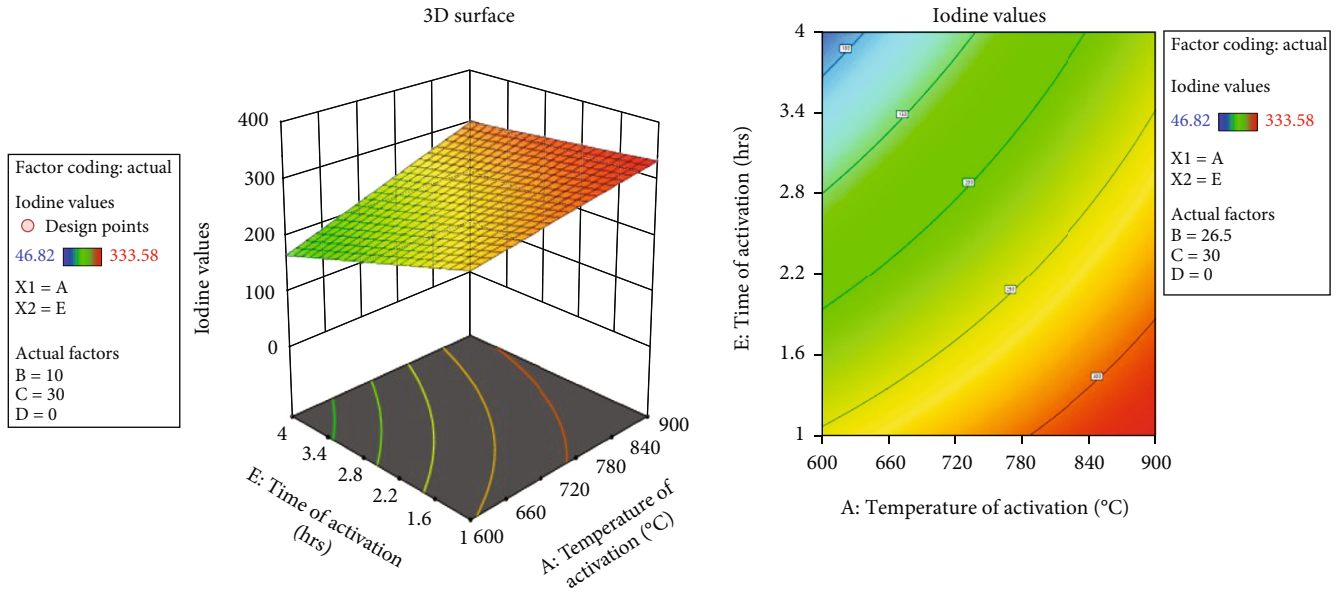

Figure 7: Surface and contour plots of the effect of pulse duration based on input parameters.

the phosphorus-potassium dihydrogen level by up to 30% *w*/*v* reduces or maintains the S/N proportion [25, 29]. Increased activating agents may cause increased drying and the dissolution of activated carbon fiber small pores, resulting in bigger pores with lower adsorption effectiveness. Similar findings have been reported in the research.

4.4. Effect of Carbonization Temperature. Figure 6 shows that more of the activated carbon fiber obtained by carbonizing hemp at 300°C is greater than that of activated carbon fiber generated without such a phase. Dissociating volatile substances from hemp structures could allow additional places for the activating chemical to deposit and provide more activation spots on the particle surface, enhancing activated carbon fiber adsorption [17, 30]. Carbonization at 400°C reduces the adsorption properties of activated carbon fiber, most likely owing to the shrinking of the carbonized charred molecule. Several investigators achieved consistent outcomes.

4.5. Effect of Activation Time. The findings of such an analysis of variance for the influence of pulse duration on the S/N proportions of the iodide values are shown in Figure 7. The experimental findings show that ACF's adsorption rate steadily rises after increasing pulse duration up to 3 h. A rise in pulse duration of up to 4 h reduces adsorption ability. Processing for 3 hours undoubtedly enhances the development of small pores that are more efficient in the adsorption mechanism. However, with longer activating durations, the walls of the small pores may break, and they become shiny and porous [31, 32].

4.6. Description of the Augmented Settings. According to the previous segment, the optimal conditions were 300°C combustions, insemination with 22.5% *w*/*v* K_2HPO_4 solution, and activating at 800°C for 3 hours at 20°C/min. Figure 8

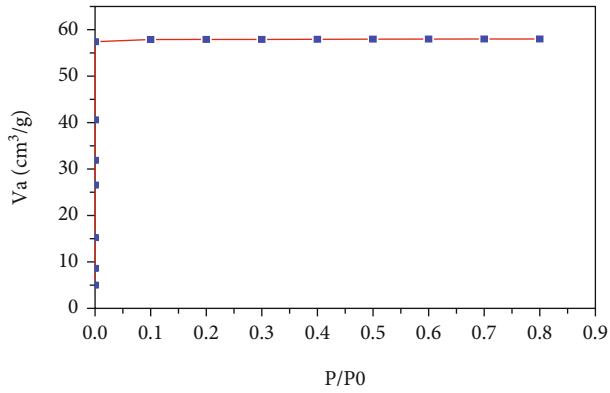

Figure 8: Nitrogen adsorption at -196°C on the activated carbon fiber prepared at optimal conditions.

depicts the nitrogen adsorbent equilibrium adsorption curves obtained at -196°C under optimum circumstances. As per the IUPAC, the resulting equilibrium adsorption curves support a category I adsorbent where most activated carbon fiber's permeability seems to be in microporous sizes [20, 33]. The MP techniques yielded the following outcomes: an appropriate surface region of 469 m^2/g, a small pore surface of 461 m^2/g, a micropore surface of 10.7 m^2/g, small pore volumes of 0.15 m^3/g, and a microporous volume of 1.24×10^2 m^3/g. When specific surface area volume data were compared, it was discovered that the majority of the permeability of a produced surface would be in the microporous range, indicating that activated carbon fiber created under optimal conditions has a very high porosity structure and is composed of small pores [34].

Figure 9 shows the microstructural images of pure and activated hemp fibers. A comparison of SEM micrographs of the ACF surface generated under optimal circumstances

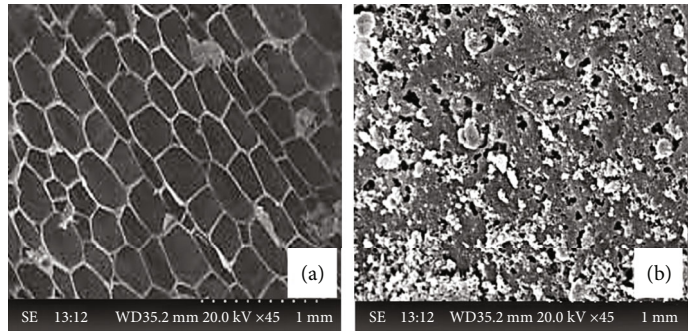

Figure 9: Microstructural images of (a) pure hemp and (b) activated carbon-based hemp.

with pure hemp shows that a significant amount of permeability is formed throughout the carbonization phases. The ACF's uneven porosity suggests a much greater surface area than created under optimum ACF processing conditions.

5. Conclusion

The activated carbon from hemp-based natural fibers was successfully formed using dipotassium hydrogen phosphate's chemical solvent, and the results were optimized through the Taguchi optimization tool. The following results were obtained.

(i) According to the previous Taguchi, the optimal conditions were 300°C combustions, insemination with 22.5% w/v K_2HPO_4 solution, and activating at 800°C for 3 hours at a rate of 20°C/min

(ii) The most significant contribution is 54.75%, followed by the rate of temperature activation at 23.35%, carbonated temperature at 10.14%, duration of stimulation at 8.82%, and H_3PO_4 concentrations at 2.94%. The results show that the activation temperature and rate of the temperature of activations are the most important elements in the current study's accomplishment of the best adsorption capacities

(iii) As per the IUPAC, the resulting equilibrium adsorption curves support a category I adsorbent where most activated carbon fiber's permeability seems to be in microporous sizes

(iv) The MP techniques yielded the following outcomes: an appropriate surface region of 469 m^2/g, a small pore surface of 461 m^2/g; a micropore surface of 10.7 m^2/g; small pore volumes of 0.15 m^3/g; and a microporous volume of 1.24×10^2 m^3/g

(v) Dissociating volatile substances from hemp structures could allow additional places for the activating chemical to deposit and provide more activation spots on the particle surface, enhancing the adsorption of activated carbon fiber

(vi) The experimental findings show that ACF's adsorption rate steadily rises after increasing pulse duration up to 3 h. A rise in pulse duration of up to 4 h reduces adsorption ability. Processing for 3 hours undoubtedly enhances the development of small pores that are more efficient in the adsorption mechanism

Data Availability

The data used to support the findings of this study are included within the article.

Conflicts of Interest

The authors declare that there are no conflicts of interest regarding the publication of this paper.

Acknowledgments

We thank and acknowledge the management of Saveetha School of Engineering, Chennai, for their support to carry out this research work.

References

[1] S. Ouajai and R. A. Shanks, "Composition, structure and thermal degradation of hemp cellulose after chemical treatments," *Polymer Degradation and Stability*, vol. 89, no. 2, pp. 327–335, 2005.

[2] N. Saba, M. T. Paridah, K. Abdan, and N. A. Ibrahim, "Effect of oil palm nano filler on mechanical and morphological properties of kenaf reinforced epoxy composites," *Construction and Building Materials*, vol. 123, pp. 15–26, 2016.

[3] V. Ganesan and B. Kaliyamoorthy, "Utilization of Taguchi technique to enhance the interlaminar shear strength of wood dust filled woven jute fiber reinforced polyester composites in cryogenic environment," *Journal of Natural Fibers*, vol. 19, no. 6, pp. 1990–2001, 2022.

[4] G. Velmurugan and K. Babu, "Statistical analysis of mechanical properties of wood dust filled jute fiber based hybrid composites under cryogenic atmosphere using Grey-Taguchi method," *Materials Research Express*, vol. 7, no. 6, 2020.

[5] M. Anbia, F. M. Nejati, M. Jahangiri, A. Eskandari, and V. Garshasbi, "Optimization of synthesis procedure for NaX zeolite by Taguchi experimental design and its application in CO_2 adsorption," *Islamic Republic of Iran*, vol. 26, pp. 213–222, 2015.

[6] A. Sharafian, K. Fayazmanesh, C. McCague, and M. Bahrami, "Thermal conductivity and contact resistance of mesoporous silica gel adsorbents bound with polyvinylpyrrolidone in contact with a metallic substrate for adsorption cooling system applications," *International Journal of Heat and Mass Transfer*, vol. 79, pp. 64–71, 2014.

[7] J. Sarkar and S. Bhattacharyya, "Application of graphene and graphene-based materials in clean energy-related devices Minghui," *Archives of Thermodynamics*, vol. 33, pp. 23–40, 2012.

[8] M. Meikandan, M. Karthick, L. Natrayan et al., "Experimental investigation on tribological behaviour of various processes of anodized coated piston for engine application," *Journal of Nanomaterials*, vol. 2022, Article ID 7983390, 8 pages, 2022.

[9] K. Renugadevi, P. K. Devan, and T. Thomas, "Fabrication of Calotropis gigantea fibre reinforced compression spring for light weight applications," *Composites Part B, Engineering*, vol. 172, pp. 281–289, 2019.

[10] V. Paranthaman, K. Shanmuga Sundaram, and L. Natrayan, "Influence of SiC particles on mechanical and microstructural properties of modified interlock friction stir weld lap joint for automotive grade aluminium alloy," *Silicon*, vol. 14, no. 4, pp. 1617–1627, 2022.

[11] S. Mishra, A. K. Mohanty, L. T. Drzal, M. Misra, and G. Hinrichsen, "A review on pineapple leaf fibers, sisal fibers and their biocomposites," *Macromolecular Materials and Engineering*, vol. 289, no. 11, pp. 955–974, 2004.

[12] J. C. dos Santos, R. L. Siqueira, L. M. G. Vieira, R. T. S. Freire, V. Mano, and T. H. Panzera, "Effects of sodium carbonate on the performance of epoxy and polyester coir- reinforced composites," *Polymer Testing*, vol. 67, pp. 533–544, 2018.

[13] R. del Rey, R. Serrat, J. Alba, I. Perez, P. Mutje, and F. X. Espinach, "Effect of sodium hydroxide treatments on the tensile strength and the interphase quality of hemp core fiber-reinforced polypropylene composites," *Polymers*, vol. 9, no. 8, pp. 6–8, 2017.

[14] A. S. Negi, J. K. Katiyar, S. Kumar, N. Kumar, and V. K. Patel, "Physicomechanical and abrasive wear properties of hemp/Kevlar/carbon reinforced hybrid epoxy composites," *Materials Research Express*, vol. 6, no. 11, 2019.

[15] L. Yan, N. Chouw, and K. Jayaraman, "Flax fibre and its composites - a review," *Composites Part B, Engineering*, vol. 56, pp. 296–317, 2014.

[16] S. J. Muthiya, L. Natrayan, S. Kaliappan et al., "Experimental investigation to utilize adsorption and absorption technique to reduce CO_2 emissions in diesel engine exhaust using amine solutions," *Adsorption Science & Technology*, vol. 2022, article 9621423, pp. 1–11, 2022.

[17] J. M. Pinheiro, S. Salústio, A. A. Valente, and C. M. Silva, "Adsorption heat pump optimization by experimental design and response surface methodology," *Applied Thermal Engineering*, vol. 138, pp. 849–860, 2018.

[18] K. R. Sumesh and K. Kanthavel, "Synergy of fiber content, Al_2O_3 nanopowder, NaOH treatment and compression pressure on free vibration and damping behavior of natural hybrid-based epoxy composites," *Polymer Bulletin*, vol. 77, no. 3, pp. 1581–1604, 2020.

[19] K. Lim, J. Kim, and J. Lee, "Comparative study on adsorbent characteristics for adsorption thermal energy storage system," *International Journal of Energy Research*, vol. 43, no. 9, pp. 4281–4294, 2019.

[20] S. Aber, A. Khataee, and M. Sheydaei, "Optimization of activated carbon fiber preparation from Kenaf using K_2HPO_4 as chemical activator for adsorption of phenolic compounds," *Bioresource Technology*, vol. 100, no. 24, pp. 6586–6591, 2009.

[21] A. Frazzica and V. Brancato, "Verification of hydrothermal stability of adsorbent materials for thermal energy storage," *International Journal of Energy Research*, vol. 43, no. 12, pp. 6161–6170, 2019.

[22] X. Du, T. Wu, F. Sun et al., "Adsorption equilibrium and thermodynamic analysis of CO_2 and CH_4 on Qinshui Basin anthracite," *Geofluids*, vol. 2019, Article ID 8268050, 14 pages, 2019.

[23] P. G. Youssef, H. Dakkama, S. M. Mahmoud, and R. K. AL-Dadah, "Experimental investigation of adsorption water desalination/cooling system using CPO-27Ni MOF," *Desalination*, vol. 404, pp. 192–199, 2017.

[24] F. Tadayon, T. Branch, S. Motahar, N. T. Branch, and O. Branch, "Application of Taguchi method for optimizing the adsorption of lead ions on nanocomposite silica aerogel," *Academic Research International*, vol. 2, pp. 42–48, 2012.

[25] K. Lim, J. Che, and J. Lee, "Experimental study on adsorption characteristics of a water and silica-gel based thermal energy storage (TES) system," *Applied Thermal Engineering*, vol. 110, pp. 80–88, 2017.

[26] K. E. N'Tsoukpoe, H. Liu, N. Le Pierrès, and L. Luo, "A review on long-term sorption solar energy storage," *Renewable and Sustainable Energy Reviews*, vol. 13, no. 9, pp. 2385–2396, 2009.

[27] J. Jänchen and H. Stach, "Adsorption properties of porous materials for solar thermal energy storage and heat pump applications," *Energy Procedia*, vol. 30, pp. 289–293, 2012.

[28] K. Linnow, M. Niermann, D. Bonatz, K. Posern, and M. Steiger, "Experimental studies of the mechanism and kinetics of hydration reactions," *Energy Procedia*, vol. 48, pp. 394–404, 2014.

[29] U. Pathak, S. Kumari, A. Kumar, and T. Mandal, "Process parametric optimization toward augmentation of silica yield using Taguchi technique and artificial neural network approach," *Ecology and Environment*, vol. 5, no. 4, pp. 294–312, 2020.

[30] K. C. Ng, H. T. Chua, C. Y. Chung et al., "Experimental investigation of the silica gel-water adsorption isotherm characteristics," *Applied Thermal Engineering*, vol. 21, no. 16, pp. 1631–1642, 2001.

[31] N. Yu, R. Z. Wang, and L. W. Wang, "Sorption thermal storage for solar energy," *Progress in Energy and Combustion Science*, vol. 39, no. 5, pp. 489–514, 2013.

[32] S. Vasta, V. Brancato, D. La Rosa et al., "Adsorption heat storage: state-of-the-art and future perspectives," *Nanomaterials*, vol. 8, no. 7, p. 522, 2018.

[33] A. S. Kaliappan, S. Mohanamurugan, and P. K. Nagarajan, "Numerical investigation of sinusoidal and trapezoidal piston profiles for an IC engine," *Journal of Applied Fluid Mechanics*, vol. 13, no. 1, pp. 287–298, 2020.

[34] L. Wang, L. Chen, H. L. Wang, and D. L. Liao, "The adsorption refrigeration characteristics of alkaline-earth metal chlorides and its composite adsorbents," *Renewable Energy*, vol. 34, no. 4, pp. 1016–1023, 2009.